Evaluation of the instantaneous profile method for the determination of the relative permeability function

Anne-Catherine Dieudonné, Robert Charlier

University of Liege, Belgium

Experimental determination of water permeability in unsaturated conditions is a critical issue. Among the existing experimental techniques, the instantaneous profile method is frequently used. When applied to bentonite-based materials, the method often shows that the water permeability–suction function significantly differs depending on the distance from the wetting face. Such behaviour has been interpreted as a consequence of structural changes in the sample which directly affect the water flow properties. In order to better understand the involved processes, a hydromechanical simulation of an infiltration test is performed. While structural changes are shown to affect the hydraulic properties, the computed water permeability–suction evolution is strongly affected by the interpretation of the raw experimental data.

Introduction

Unsaturated fluid flow is important in many engineering applications. For instance, a proper estimation of the time required to ultimately saturate bentonite buffers under *in situ* conditions is an important stake for the safe design of geological repositories for radioactive waste. In this context, good characterization and modelling of both water retention behaviour and unsaturated water flow are of paramount importance.

Yet, experimental determination of unsaturated water permeability is a critical issue. Among the different experimental techniques, the instantaneous profile method (Daniel, 1982) has been frequently used to determine the permeability of unsaturated materials (Cui *et al.*, 2008; Ye *et al.*, 2009; Wang *et al.*, 2013a; Schanz, 2016). According to the method, a cylindrical sample is wetted from one extremity and the evolution of relative humidity is monitored over time at different heights of the sample. The results are plotted in terms of isochrones of suction and water content at different times. In order to determine the permeability, the hydraulic gradient and liquid flux are also computed.

When applied to bentonite-based materials, the instantaneous profile method often shows that the water permeability–suction function significantly differs depending on the considered distance from the wetting face. Such behaviour has been interpreted as a consequence of structural changes in the sample which directly affect the water flow properties. In order to better understand the involved processes, a coupled hydromechanical simulation of the infiltration test is performed in this paper. The determination of the relative permeability function by means of the instantaneous profile method is then discussed.

Hydromechanical formulation for bentonite-based materials

The theoretical framework is composed of two balance equations, namely the balance of momentum and water mass balance equations. The stress equilibrium equation is expressed as:

$$\nabla \cdot \boldsymbol{\sigma_t} + \boldsymbol{b} = \boldsymbol{0}$$

where $\boldsymbol{\sigma_t}$ is the total (Cauchy) stress tensor and $\boldsymbol{b}$ is the body force vector. The mass balance equation for water is given by:

$$\frac{\partial}{\partial t}(\rho_w \phi S_r) + \nabla \cdot (\rho_w \boldsymbol{q_w}) = Q_w$$

where ρ_w is the bulk density of liquid water, ϕ is the porosity, S_r is the degree of saturation, Q_w represents any external supply of water, and $\boldsymbol{q_w}$ is the Darcy flow. It is related to the water pressure u_w through:

$$\boldsymbol{q_w} = -\frac{k_{rw}(S_r) \cdot K_w}{\mu_w}(\nabla u_w + \rho_w \boldsymbol{g})$$

where μ_w is water dynamic viscosity, K_w is the water permeability in fully saturated conditions ($S_r = 1$) and k_{rw} is the so-called relative permeability function and is a function of the degree of saturation S_r according to:

$$k_{rw} = S_r^{n_k}$$

with n_k a model parameter. Kozeny-Carman law is extended to account for the double-structure of compacted bentonite-based materials, so that the saturated water permeability K_w is a function of the macrostructural void ratio $e_M = e - e_m$ (with e the total void ratio and e_m the microstructural void ratio) according to:

$$K_w = K_{W0}\frac{(1-e_{M0})^M}{e_{M0}^N}\frac{e_M^N}{(1-e_M)^M}$$

with K_{W0} a reference permeability measured on a material with a reference macrostructural void ratio e_{M0}, and N and M two model parameters. The microstructural void ratio is not fixed but evolves with the water ratio $e_w = S_r \cdot e$ according to Dieudonne *et al.* (2014) and Della Vecchia *et al.* (2015):

$$e_m = \beta_0 e_w^2 + \beta_1 e_w + e_{m0}$$

where e_{m0} is the microstructural void ratio for the dry material, and β_0 and β_1 are parameters quantifying the swelling potential of the microstructure. The water retention model developed by Dieudonne *et al.* (2016) is adopted. The model considers adsorbed water in the microstructure and capillary water in the aggregate-porosity. Accordingly, the degree of saturation is given by:

$$S_r = \frac{e_m}{e}\exp[-(C_{ads}s)^{n_{ads}}] + \frac{e-e_m}{e}\left\{1+\left[(e-e_m)\frac{s}{A}\right]^n\right\}^{-m}$$

where C_{ads} and n_{ads} are material parameters governing the microstructural water retention mechanism, A, m and n are material parameters governing the macrostructural water retention mechanism, and s is suction.

Finally, the Barcelona Basic Model (Alonso *et al.*, 1990) is used to reproduce the mechanical behaviour of the material.

Numerical modelling of an infiltration test

Description of the test

Wang *et al*. (2013a) carried out an infiltration test on a compacted mixture of MX-80 bentonite and sand, with respective proportions of 70/30 in dry mass. The specimen (250-mm high and 50 mm in diameter) was compacted to a dry density of 1.67 Mg/m³ and an initial water content of 11%. It was then introduced in a constant-volume cylindrical cell of the same diameter for the infiltration test. Four relative humidity sensors were installed every 50 mm along the sample as shown in Fig. 1. The initial relative humidity of the specimen was measured equal to 65 MPa. Water supply was done at atmospheric pressure from the bottom base. The top cover allows air expulsion but limited water evaporation.

Features of the analysis

A hydromechanical model of the infiltration test is realized. The analysis assumes one-dimensional axisymmetric conditions around the longitudinal axis of the sample. An initial isotropic stress state of 0.1 MPa is considered in the whole sample, the effects of gravity being neglected. On the other hand, the initial suction in the sample is equal to 65 MPa. Finally, water injection in the bentonite sample is modelled by imposing the water pressures at the bottom of the sample equal to 0.1 MPa. No water flow is allowed at the top of the sample.

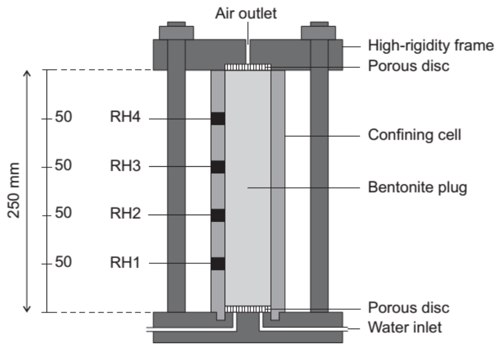

Fig. 1: Representation of the experimental set-up used for the infiltration test (Wang *et al.*, 2013a). RH1 to RH4 denote the relative humidity sensors.

The parameters of the hydromechanical model were calibrated against experimental data from Gatabin *et al.* (2008), Wang *et al.* (2013b) and Gatabin *et al.* (2016). They are given in Table 1. Finally, the exponent n_k of the relative permeability law is calibrated by best-fitting the responses of two relative humidity sensors, namely RH2 and RH3, located at distances of 100 and 150 mm from the injection front. Consequently, the model is validated by comparing the experimental and numerical results for the two other sensors, namely RH1 and RH4. A value of $n_k = 3.4$ is used in the reference analysis.

Table 1: Hydromechanical parameters of the MX-80 bentonite/sand mixture.

Microstructure evolution model			
e_{m0}	0.29		
β_1	0.18		
β_0	0.1		
Water retention model			
A (MPa)	0.2	C_{ads} (MPa^{-1})	0.0053
n	3	n_{ads}	0.79
m	0.15		
Water flow model			
K_{w0} (m²)	2.5 x 10^{-20}	N	2
e_{M0}	0.31	M	0.2
Barcelona Basic Model			
κ	0.025	$\lambda(0)$	0.12
κ_s	0.073	p_0^* (MPa)	1.40
ν	0.35	p_c (MPa)	0.01
$c(0)$ (MPa)	0.1	r	0.8

k	0.046	ω (MPa^{-1})	0.09
ϕ (°)	25		

Numerical results

Fig. 2 presents the evolution through of the relative humidity measured at different heights of the sample. The numerical results are compared to the experimental results.

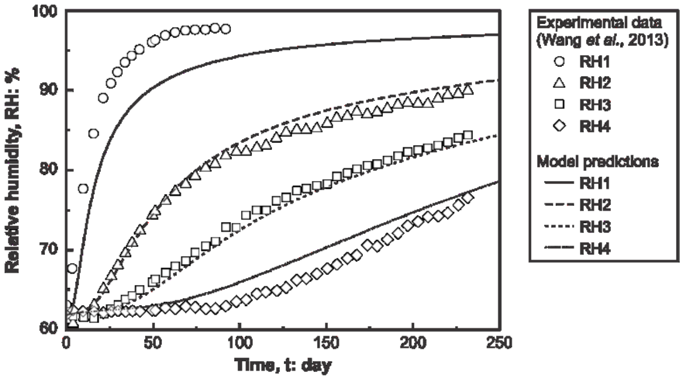

Fig. 2: Evolution of relative humidity during water infiltration. Comparison between experimental data (Wang *et al.*, 2013a) and model predictions.

As soon as hydration starts, an increase in relative humidity is detected by the sensor RH1, located at a distance of 50 mm from the wetting face. As water injection proceeds, the sensors RH2, RH3 and RH4 located at increasing distances from the bottom progressively exhibit an increase in relative humidity. As observed in Fig. 2, the hydration rate is all the more important that the considered point is situated close to the injection water face. The progressive increase of relative humidity measured by the different sensors is well captured by the numerical model. A somewhat weaker agreement is obtained for RH1 which is located the closest from the injection front. Indeed, the very fast reaction of this sensor is not well reproduced numerically. This discrepancy of the model could be explained either by the assumed equilibrium between the microstructural and macrostructural levels, or by the fact that the infiltration cell is different from the compaction cell. In any case, the difference between the observed and modelled results should be balanced by the accuracy of the relative humidity sensors which is generally of the order of 1 to 3 %.

Evaluation of the instantaneous profile method for the determination of the relative permeability function

The instantaneous profile method has often been used to interpret infiltration tests and determine the water permeability of unsaturated porous materials. By monitoring of the injected water volume and the evolution of the relative humidity at different distances from the wetting front, the water permeability may be expressed as a function of suction. Fig. 3 presents the evolution of the water permeability with suction predicted by the numerical model. Note that the different permeability values are obtained at four different Gauss points of the mesh. For the sake of comparison, the permeabilities computed by Wang *et al.* (2013a) using the instantaneous profile method are also represented.

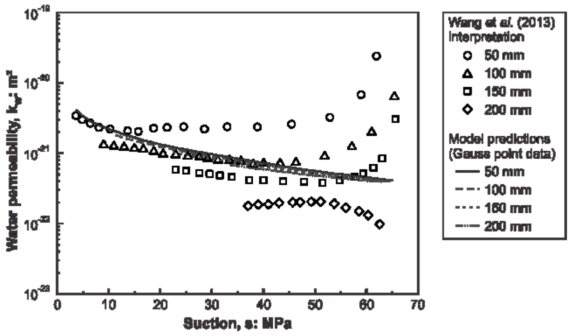

Fig. 3: Water permeability versus. Comparison between Wang *et al.* (2013a) interpretation and the values obtained from the numerical model. Water permeabilities are obtained directly at different Gauss points.

Despite the good performance of the numerical model in reproducing the evolution of relative humidity in the sample, a very bad agreement is apparently obtained in terms of unsaturated water permeability. Indeed, Wang *et al.* (2013a) showed that the permeability evolution strongly depends on the considered height. At the bottom of the sample, an important decrease in permeability is observed between 65 MPa and 50 MPa of suction. The permeability is then relatively stable with decreasing suctions, although a slight increase is observed below 15 MPa. On the contrary, an increase in permeability is detected in the high suction range for the sensor located the furthest from the injection side. This trend is not reproduced by the numerical model which predicts a continuous increase of the water permeability with suction, regardless the distance from the wetting face. In addition, the evolution of the water permeability is less significant than the one predicted by Wang *et al.* (2013a) using the instantaneous profile method.

In order to determine the permeability of the partially saturated porous media, the hydraulic gradient i and the water flux q_w must be computed. In particular, the hydraulic gradient i is calculated as the slope of the isochrone. It reads

$$i(t) = \frac{\Delta s}{\Delta y}\bigg|_t$$

s and y being expressed in the same length units. On the other hand, using the water retention curve, the relative humidity profile can be converted into a water content profile. Considering the volumetric water content profiles at different times, the water flux can be determined according to

$$q_w(y_i) = A\frac{\int_{y_i}^{H} \theta(t + \Delta t)\, dy \; - \int_{y_i}^{H} \theta(t)\, dy}{\Delta t}$$

where A is the surface area of the sample face, H is the sample height and θ is the volumetric water content. Then, knowing both hydraulic gradient and water flux, the permeability is obtained as (Daniel, 1982)

$$k_w = -\frac{1}{A}\frac{q_w(y_i)}{\frac{1}{2}(i_t + i_{t+\Delta t})}$$

It can be computed as a function of suction at different heights of the sample corresponding to the positions of the relative humidity sensors. Here, the evolutions of relative humidity at 50 mm, 100 mm, 150 mm and 250 mm from the wetting end are used as input data for the instantaneous profile method (Fig. 4). The evolutions of water permeability computed in this way are in good agreement with those determined by Wang *et al.* (2013a), both qualitatively and quantitatively.

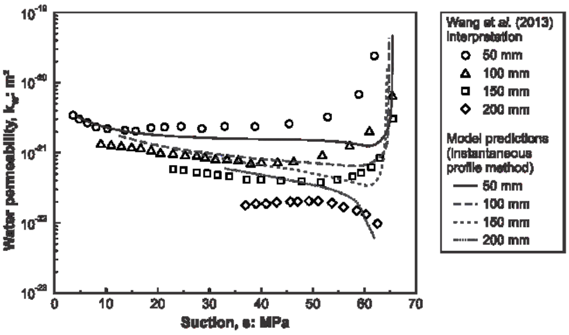

Fig. 4: Water permeability versus suction. Comparison between Wang *et al.* (2013a) interpretation and the reinterpretation of the numerical results.

Conclusions

The instantaneous profile method is frequently used to determine the permeability of unsaturated soils. When applied to bentonite-based materials, it shows that the water permeability–suction function significantly differs depending on the distance from the wetting face. In this paper, a hydromechanical simulation of an infiltration test is performed. We show that the evolution of water permeability with suction as computer by the instantaneous profile method differs from the permeability values obtained at the Gauss points. In particular, the instantaneous profile method tends to overestimate the changes of unsaturated permeability during hydration. While infiltration column tests provide valuable and necessary data to assess the hydration kinetics of bentonite-based materials, their interpretation using the instantaneous profile method should be taken with caution.

References

Alonso EE, Gens A, Josa A (1990) A constitutive model for partially saturated soils. Géotechnique 40(3): 405-430

Cui YJ, Tang AM, Loiseau C, Delage P (2008) Determining the unsaturated hydraulic conductivity of a compacted sand–bentonite mixture under constant-volume and free-swell conditions. Physics and Chemistry of the Earth 33: S462-S471

Daniel DE (1982) Measurement of hydraulic conductivity of unsaturated soils with thermocouple psychrometers. Soil Science Society of America Journal 46(6): 1125–1129.

Della Vecchia G, Dieudonne AC, Jommi C, Charlier R (2015) Accounting for evolving pore size distribution in water retention models for compacted clays. International Journal for Numerical and Analytical Methods in Geomechanics 39(7): 702-723.

Dieudonne AC, Charlier R, Levasseur S, Della Vecchia G, Jommi C (2014) Evolution of clay fabric and water retention properties along hydromechanical stress paths. Numerical Methods in Geotechnical Engineering, Proceedings of the 8th European Conference on Numerical Methods in Geotechnical Engineering, NUMGE 2014: 971–975

Dieudonne AC, Gatabin C, Talandier J, Collin F, Charlier R (2016) Water retention behaviour of compacted bentonites: experimental observations and constitutive model. 3rd European Conference on Unsaturated Soils – "E-UNSAT 2016". E3S Web of Conferences 9, 11012. doi: 10.1051/e3sconf/20160911012

Gatabin C, Talandier J, Collin F, Charlier R, Dieudonne AC (2016) Competing effects of volume change and water uptake on the water retention behaviour of a compacted MX-80 bentonite/sand mixture. Applied Clay Science 121-122: 57-62.

Gatabin C, Touze G, Imbert C, Guillot W, Billaud P (2008) ESDRED project, Module 1-selection and THM characterization of the buffer material. Proceedings of the International Conference Underground Disposal Unit Design & Emplacement Processes for a Deep Geological Repository, Prague.

Schanz T (2016) Transient boundary conditions in the frame of THM-processes at nuclear waste repositories. 3rd European Conference on Unsaturated Soils – "E-UNSAT 2016". E3S Web of Conferences 9, 03001. doi: 10.1051/e3sconf/20160903001

Wang Q, Cui YJ, Tang AM, Barnichon JD, Saba S, Ye WM (2013a) Hydraulic conductivity and microstructure changes of compacted bentonite/sand mixture during hydration. Engineering Geology 164: 67-76.

Wang Q, Tang AM, Cui YJ, Delage P, Barnichon JD, Ye WM (2013b) The effects of technological voids on the hydro-mechanical behaviour of compacted bentonite–sand mixture. Soils and Foundations 53(2): 232-245

Ye WM, Cui YJ, Qian LX, Chen B (2009) An experimental study of the water transfer through confined compacted GMZ bentonite. Engineering Geology 108(3-4): 169-176.